Vertical Variability of Aerosols and Water Vapor Over the Southern Great Plains

R. A. Ferrare
National Aeronautics and Space Administration
Langley Research Center
Hampton, Virginia

J. A. Ogren
National Oceanic and Atmospheric Administration
Climate Monitoring and Diagnostics Laboratory
Boulder, Colorado

D. D. Turner
Pacific Northwest National Laboratory
Richland, Washington

E. Andrews
Cooperative Institute for Research in Environmental Sciences
University of Colorado
Boulder, Colorado

M. Clayton and V. Brackett
Science Applications International Corporation
National Aeronautics and Space Administration
Langley Research Center
Hampton, Virginia

A. Marshak
National Aeronautics and Space Administration
Goddard Space Flight Center
Greenbelt, Maryland

T. P. Tooman and J. E. M. Goldsmith
Sandia National Laboratories
Livermore, California

A. B. Davis
Los Alamos National Laboratory
Los Alamos, New Mexico

Abstract

We use Raman lidar profiles of water vapor mixing ratio, relative humidity, aerosol backscattering, and aerosol extinction acquired over the last few years to study the variability of aerosols and water vapor over the Atmospheric Radiation Measurement (ARM) Southern Great Plains (SGP) site in Northern Oklahoma. Autocorrelation functions computed as a function of altitude from these profiles show large mesoscale variability in the aerosol backscattering and extinction profiles. Four day back trajectories are computed using the National Oceanic and Atmospheric Administration (NOAA) Hybrid Single-Particle Lagrangian Integrated Trajectory (HYSPLIT) model for this same period. A statistical clustering method is used to classify the trajectories into large-scale atmospheric transport patterns. The Raman lidar measurements are combined with these trajectory analyses to show how the vertical profiles of water vapor and aerosol extinction vary with these transport patterns, and to show the relationships between these transport patterns and aerosol optical thickness and precipitable water vapor.

We also update our comparisons of the Raman lidar aerosol extinction profiles with aerosol extinction profiles derived from airborne in situ aerosol profiling (IAP) measurements. The IAP aerosol extinction measurements are typically 20-40% lower than the corresponding measurements from the lidars. Differences may be due to corrections applied to the IAP data to adjust the dry aerosol scattering to ambient relative humidity as well as to account for scattering by supermicron particles. Modifications to

the IAP measurements to include aerosol scattering at a single elevated relative humidity will hopefully help reduce these differences.

Introduction

Two of the primary objectives of ARM are: (1) relate observations of radiative fluxes and radiances to the atmospheric composition and (2) use these relations to develop and test parameterizations to accurately predict the atmospheric radiative properties. Measurements of water vapor are especially important in characterizing the atmospheric state because uncertainties in the water vapor field dominate the spectral effects in the atmospheric window region (8.3-12.5 um). Radiosonde profiles of water vapor have limited temporal resolution and often have insufficient accuracy (Revercomb et al. 2003). Moreover, radiosondes generally have inadequate temporal and/or spatial resolution to observe small-scale water vapor variability and to relate this variability to mesoscale and synoptic scales. We discuss how the Cloud and Radiation Testbed (CART) Raman lidar (CARL) (Goldsmith et al. 1998) can provide water vapor measurements that examine water vapor variability across a wide range of atmospheric scales

Vertical profiles of aerosol properties are required for the computation of radiative flux profiles. ARM has supported the development of systematic and routine measurements of aerosols at the ARM SGP site, including measurements by surface in situ instruments as well as by lidars and periodic aircraft-borne in situ sensors. These efforts have primarily focused on measurements of aerosol optical thickness (AOT), retrievals of vertical profiles of aerosol scattering and extinction, and surface measurements of aerosol optical and physical characteristics. CARL has been used to measure profiles of aerosol extinction as well as water vapor (Turner et al. 2001) and for identifying occurrences of large vertical variations in aerosol intensive (e.g. size, shape, composition) properties through measurements of the aerosol extinction/backscattering ratio ("lidar ratio") (Ferrare et al. 2001). The ARM IAP measurement program (Andrews et al. 2001) is a unique activity where routine measurements of aerosol scattering, backscattering, and absorption are acquired by in situ instruments on a small aircraft flown two to three times per week on a long term (i.e., multi-year) basis. We compare the CARL and IAP water vapor and aerosol measurements.

Instruments

CARL autonomously measures profiles of aerosols, optically thin clouds, and water vapor in the low to mid troposphere throughout the diurnal cycle (Goldsmith et al. 1998). A tripled Nd:YAG laser, operating at 30 Hz with 350-400 millijoule pulses, is used to transmit light at 355 nm. A telescope collects the light backscattered by molecules and aerosols at the laser wavelength and the Raman scattered light from water vapor (408 nm) and nitrogen (387 nm) molecules. Profiles of water vapor mixing ratio, relative humidity, aerosol backscattering, and aerosol extinction are derived routinely using a set of automated algorithms (Turner et al. 2002). Water vapor mixing ratio profiles are computed using the ratio of the Raman water vapor signal to the Raman nitrogen signal. Relative humidity profiles are computed using these profiles and the temperature profiles from the collocated Atmospheric Emitted Radiance Interferometer (AERI) (Revercomb et al. 1993). The water vapor mixing ratio profiles are integrated with altitude to derive precipitable water vapor (PWV). Profiles of

aerosol scattering ratio are derived using the Raman nitrogen signal and the signal detected at the laser wavelength. Aerosol volume backscattering cross section profiles are then computed using the aerosol scattering ratio and molecular scattering cross section profiles derived from atmospheric density data. Aerosol extinction profiles are computed from the derivative of the logarithm of the Raman nitrogen signal with respect to range. AOT is derived by integration of the aerosol extinction profile with altitude.

The IAP suite of instruments, developed at NOAA/CMDL, consists of a nephelometer to measure forward and backward scattering by aerosols at three wavelengths (450, 550, and 700nm), and a particle/soot absorption photometer (PSAP) to measure light absorption at a single wavelength (adjusted to 550 nm) (Andrews et al. 2001). The air sample is heated if necessary so that these measurements are made at a relative humidity less than about 40%. A 1-μm impactor removes supermicron (i.e., diameter >1 μm) particles so that only fine particle scattering and absorption are measured. A Vaisala Humicap 50Y capacitive sensor measures ambient relative humidity. These instruments are deployed on board a Cessna C-172N aircraft. Flights are made two or three times each week, during daytime hours at nine level flight legs over (or near) the ARM Central Facility at altitudes from about 0.2 to 3.7 km above ground level.

Trajectory Analysis

Four-day back trajectories were computed using the NOAA HYSPLIT4 model (http://www.arl.noaa.gov/ready/hysplit4.html, NOAA Air Resources Laboratory, Silver Spring, Maryland). These trajectories were computed at several altitudes every three hours for the period between January 2000 and December 2002. A cluster analysis method (Dorling et al. 1992) was used to objectively group these trajectories and to discriminate distinct flow patterns and large-scale circulation patterns (Stohl 1998). Figure 1 shows clusters of back trajectories computed at 600 m above the surface for the summer (June, July, and August) months during this period. The percentages of trajectories that were represented by the various clusters are shown. Note that over two-thirds of the trajectories show air parcels originating southeast of the SGP site; most of these trajectories originated over the Gulf of Mexico. Figure 1 also shows that these trajectories were also confined to altitudes below about 1.5 km. Few (<15%) of the trajectories were observed to originate northwest of the SGP site. In contrast, Figure 2 shows that nearly two-thirds of the trajectories originated to the west or northwest of the SGP site during the winter; less than 5% of the trajectories originated from southeast of the site.

Profiles of average aerosol extinction and water vapor mixing ratio corresponding to the various trajectory groups were computed from the CARL data and are also shown in Figures 1 and 2. Those trajectories that originated from the southeast and east of the SGP site had the highest aerosol extinction and water vapor amounts regardless of season; conversely, those trajectories originating from the west and northwest typically had the smallest aerosol extinction and water vapor amounts. This result is further illustrated in Figures 3 and 4. Figure 3 (left panel) shows trajectory clusters computed when CARL measured aerosol optical thickness (355 nm) greater than 0.4, which occurred 24% of the time, and Figure 3 (right panel) shows trajectory clusters computed when CARL measured aerosol optical thickness less than 0.1, which occurred 19% of the time. Figure 4 shows similar results for precipitable water vapor. These results show that air parcels originating from the east and southeast typically occurred during the summer and had the highest aerosol extinction and water vapor amounts, while

those trajectories originating from the west and northwest typically occurred during the winter and had the lowest aerosol extinction and water vapor amounts. These observations of high aerosol extinction and water vapor amounts associated with southeasterly and easterly trajectories is consistent with increased aerosol extinction associated with hygroscopic growth of aerosol particles as with the transport of air masses from urban/industrial areas.

Water Vapor and Aerosol Variability

We have begun to examine aerosol and water vapor variability using a time series of over 54,000 CARL profiles acquired during 2000 and 2001. This set corresponds to cloud-free conditions below 3 km observed over the SGP site. Figure 5 (left panel) shows the series of 10-minute averaged water vapor measurements acquired at an altitude of 0.47 km during this period. The annual variability is clearly seen in this figure. An indication of the diurnal and mesoscale variabilities of water vapor can be seen in the inset in Figure 5, which shows an expanded view of the data acquired over the week between November 25 and December 2, 2000. The right panel in Figure 5 shows first and second order temporal structure functions for water vapor mixing ratio at 0.47 and 2.0 km. Changes in the slopes of these structure functions at around 8-10 hours indicate a scale break that corresponds to a spatial scale of about 180-360 km for wind speeds of 5 to 10 m/s. This scale break is associated with the transition to a stationary regime also found from the multi-filter rotating shadowband radiometer (MFRSR) aerosol optical thickness measurements (Alexandrov et al. 2003). Note also the scale break associated with the seasonal scales around 1000-2000 hours. Inset to the right panel in Figure 5 illustrates the structure function exponents, $\zeta(q)$, for moments from 1 to 5. The power law spectral slope $\beta = \zeta(2) + 1$ varies between 1.8-2.0, similar to the range found using aircraft in situ water vapor measurements acquired in the extratropical free troposphere (Cho et al. 2000). In contrast to these lidar data, their spectral exponent increased with altitude. Figure 6 shows the corresponding time series of aerosol extinction measurements, structure functions, and structure function slopes. Here changes in the slopes of these structure functions at around 6-8 hours indicate a scale break that corresponds to a spatial scale of about 200-280 km for wind speeds of 5 to 10 m/s. The power law spectral slope $\beta = \zeta(2) + 1$ varies between 1.6-1.8 and also decreased with altitude.

Autocorrelation functions for water vapor mixing ratio, relative humidity, aerosol backscattering, and aerosol extinction were computed at various altitudes using the 10-minute resolution CARL data acquired during 2000 and 2001. Figure 7 shows these autocorrelation functions computed for various altitudes. Water vapor shows less variability than aerosol backscattering and extinction, particularly near the surface. Temperature variations apparently produce a large diurnal variability in the relative humidity, since there appears to be much less diurnal variability in the water vapor mixing ratio. This diurnal variability in relative humidity also leads to the diurnal variability in the aerosol extinction due to the hygroscopic growth of the aerosols as discussed above (Ferrare et al. 2003). For a given temporal lag and altitude, the autocorrelation function for water vapor is considerably larger than for aerosol backscattering and extinction, which indicates that there was less mesoscale variability in water vapor mixing ratio than aerosol backscattering and extinction. A recent study using ground, aircraft, and spaceborne measurements also found significant and general mesoscale variability in aerosol scattering (Anderson et al. 2003).

Comparison of CARL and IAP Measurements

We have also continued our comparisons of CARL and IAP measurements, using data acquired between May 2000 and December 2002. As shown in Figure 8, relative humidity derived from the CARL and IAP data show generally very good agreement, with average differences of about 5%. Aerosol extinction derived from the IAP data appears to be about 30-40% smaller, on average, than corresponding values from the Raman lidar data. The IAP aerosol extinction profile (dry) represents the sum of dry aerosol scattering and absorption at 550 nm. In order to compare with the Raman lidar extinction profile corresponding to ambient relative humidity, two corrections were applied to the IAP (dry) profile. The nephelometer aerosol scattering and resulting extinction profiles were scaled to the ambient relative humidity using a humidification (i.e., hygroscopic growth) factor derived from measurements of light scattering as a function of relative humidity made at the surface (Andrews et al. 2001). (No attempt was made to correct PSAP measurements of dry aerosol absorption to ambient relative humidity.) In addition, since the IAP measurements do not account for scattering from supermicron (>1 micron) particles, which is on average about 15% of the aerosol light scattering at 550nm at the surface (Sheridan et al. 2001), an additional increase of 15% was applied to derive an estimate of the IAP aerosol extinction profiles at ambient conditions. The CARL aerosol extinction profiles at 355 nm were scaled to 550 nm using the wavelength dependence of aerosol scattering measured between 450 and 550 nm derived from the IAP measurements. Currently, the reasons for the differences between aerosol extinction derived from the CARL and IAP are not known, but may be related to the corrections applied to the IAP data to adjust the dry aerosol scattering to ambient relative humidity as well as to account for scattering by supermicron particles. Note also that the Raman lidar measurements of aerosol extinction below about 800 m are derived by assuming that the aerosol extinction/backscatter ratio measured above 800 m also applies below this level (Ferrare et al. 2001). Future IAP measurements will include aerosol scattering at a single elevated relative humidity to help reduce the uncertainties associated with the humidification correction.

Corresponding Author

Richard Ferrare, Richard.A.Ferrare@nasa.gov, (757) 864-9443

References

Alexandrov, M., A. Marshak, B. Cairns, A. Lacis, and B. Carlson, 2003: Scaling properties of aerosol optical thickness fields retrieved from ground-based and satellite measurements. *J. Atmos. Sci*., submitted.

Anderson, T. L., R. J. Charlson, D. M. Winker, J. A. Ogren, and K. Holmen, 2003: On the generality of mesoscale variations of tropospheric aerosols. *J. Atmos. Sci*., 60, 119-136.

Andrews E., P. J. Sheridan, and J. A. Ogren, 2001: In situ aerosol profiles over the Southern Great Plains CART Site. In *Proceedings of the Eleventh Atmospheric Radiation Measurement (ARM) Science Team Meeting*, ARM-CONF-2001. U.S. Department of Energy, Washington, D.C. Available URL: http://www.arm.gov/docs/documents/technical/conf_0103/andrews-e.pdf

Cho, J. Y. N., R. E. Newell, and G.W. Sachse, 2000: Anomalous scaling of mesoscale tropospheric humidity fluctuations. *Geophys. Res. Lett*., **27**, 377-380.

Dorling, S. R., T. D. Davies, and C. E. Pierce, 1992: Cluster Analysis: A Technique for Estimating the Synoptic Meteorological Controls on Air and Precipitation Chemistry – Method and Applications. *Atm. Environ*., 26A, No. 14, 2575-2581.

Ferrare, R. A., D. D. Turner, L. A. Heilman, O. Dubovik, and W. Feltz, 2001: Raman lidar measurements of the aerosol extinction-to-backscatter ratio over the Southern Great Plains. *J. Geophys. Res*., **106**, 20,333-20,347.

Ferrare, R. A., E. V. Browell, S. Ismail, J. Barrick, G. Diskin, S. Kooi, L. H. Brasseur, V. G. Brackett, M. Clayton, B. Lesht, L. Miloshevich, J. Podolske, F. Schmidlin, and D. D. Turner, 2003: Lidar characterizations of water vapor measurements over the arm SGP site. *AMS Conference on "Observing and Understanding the Variability of Water in Weather and Climate.*"

Goldsmith, J. E. M., F. H. Blair, S. E. Bisson, and D. D. Turner, 1998: Turn-Key Raman lidar for profiling atmospheric water vapor, clouds, and aerosols. *Appl. Opt*., **37**, 4979–4990.

Revercomb, H., et al., 2003: *Bull. Amer. Meteor. Soc*., **84**, 217-236.

Revercomb, H., F. A. Best, R. G. Dedecker, T. P. Dirkx, R. A. Herbsleb, R. O. Knuteson, J. F. Short, and W. L. Smith, 1993: Atmospheric emitted radiance interferometer (AERI) for ARM. Preprints. *Fourth Symp. on Global Climate Change Studies, Amer. Meteor. Soc*., 46-49, Anaheim, California.

Sheridan, P. J., D. J. Delene, and J. A. Ogren, 2001: Four years of continuous surface measurements from the Department of Energy's Atmospheric Radiation Measurement Program Southern Great Plains Cloud and Radiation Testbed site. *JGR*, **106**, No. D18, 20,735-20,747.

Stohl, A., 1998: Computation, accuracy, and applications, of trajectories – A Review and Bibliograph. *Atm. Environ*., **32**, No. 6, 947-966.

Turner, D. D., R. A. Ferrare, and L. A. Brasseur, 2001: Average aerosol extinction and water vapor profiles over the Southern Great Plains. *Geophys. Res. Letters*, **28**, 4441-4444.

Turner, D. D., R. A. Ferrare, L. A. Heilman, W. F. Feltz, and T. Tooman, 2002: Automated retrievals of water vapor and aerosol profiles over Oklahoma from an operational Raman lidar. J. *Atmos. Oceanic Tech*., **19**, 37-50.

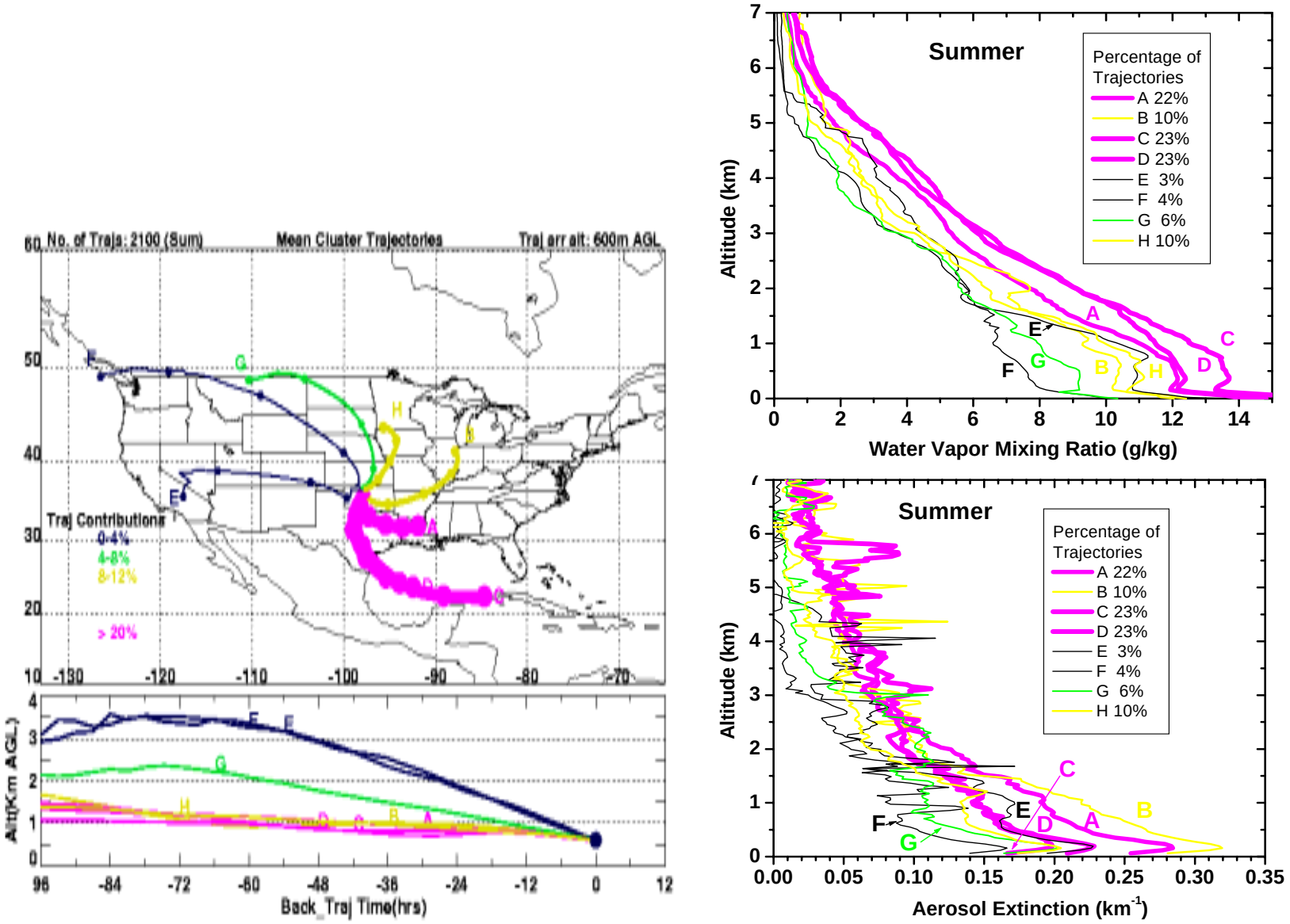

Figure 1. (Left) Mean cluster trajectories arriving over the ARM SGP site during the summer. (Right) Average water vapor and aerosol extinction profiles derived from CARL data corresponding to the mean cluster trajectories.

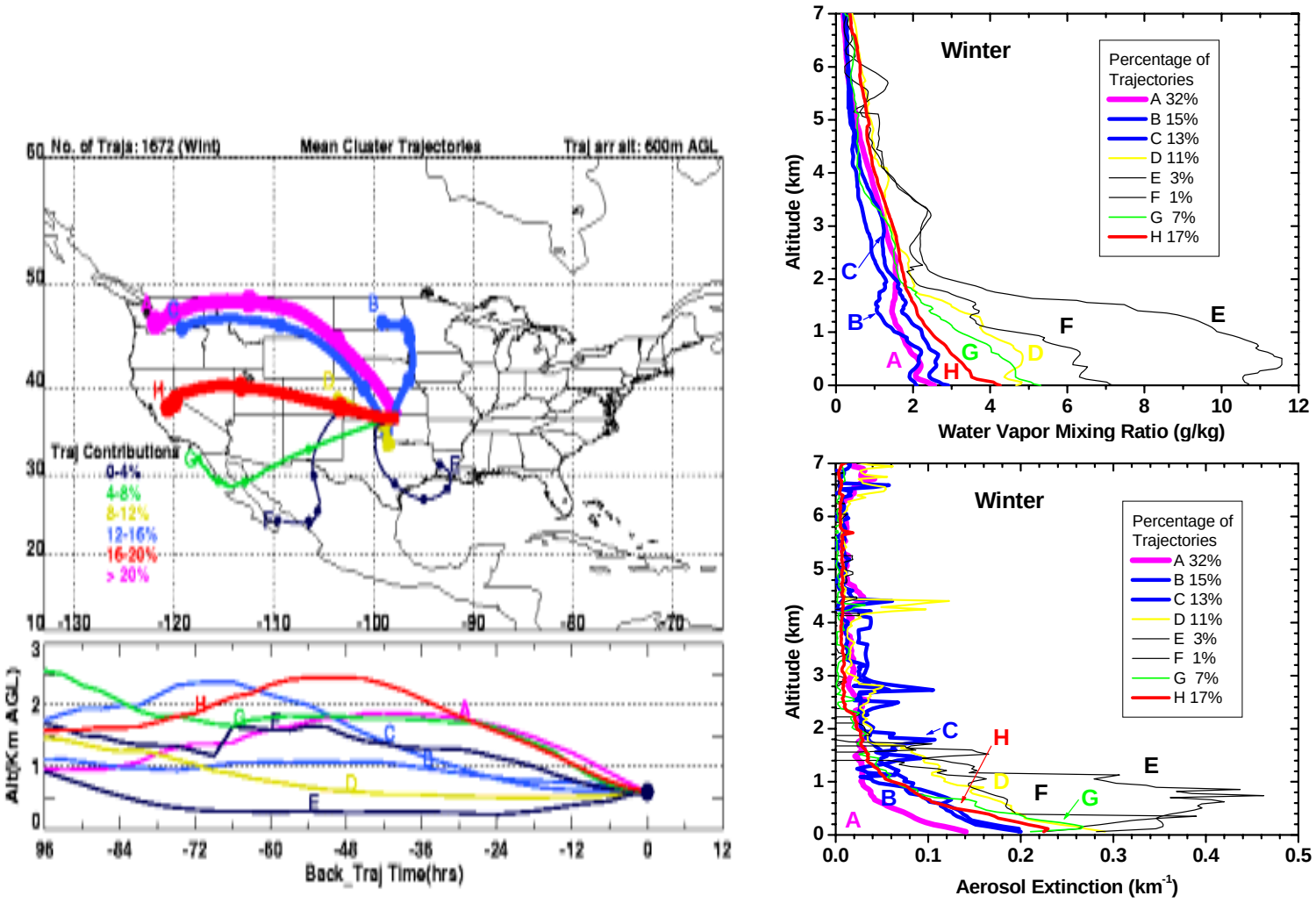

Figure 2. Same as Figure 1 except for winter.

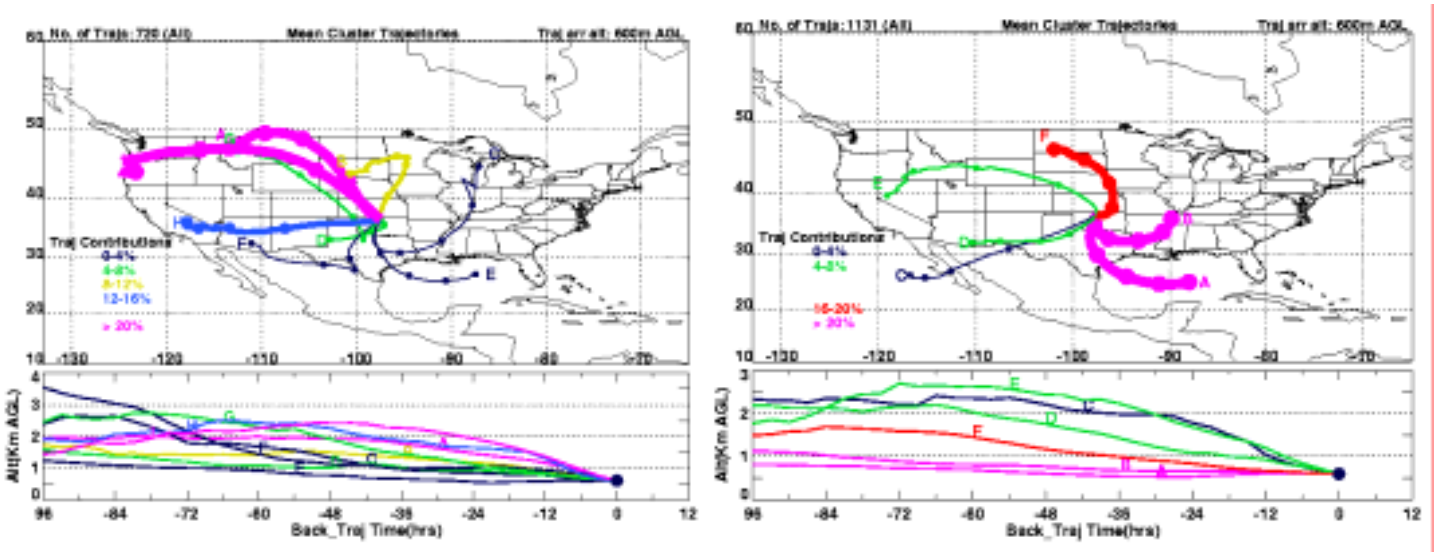

Figure 3. (Left) Mean trajectory clusters for cases when CARL measured AOT (355 nm) <0.1; (Right) Mean trajectory clusters for cases when CARL measured AOT (355 nm) >0.4.

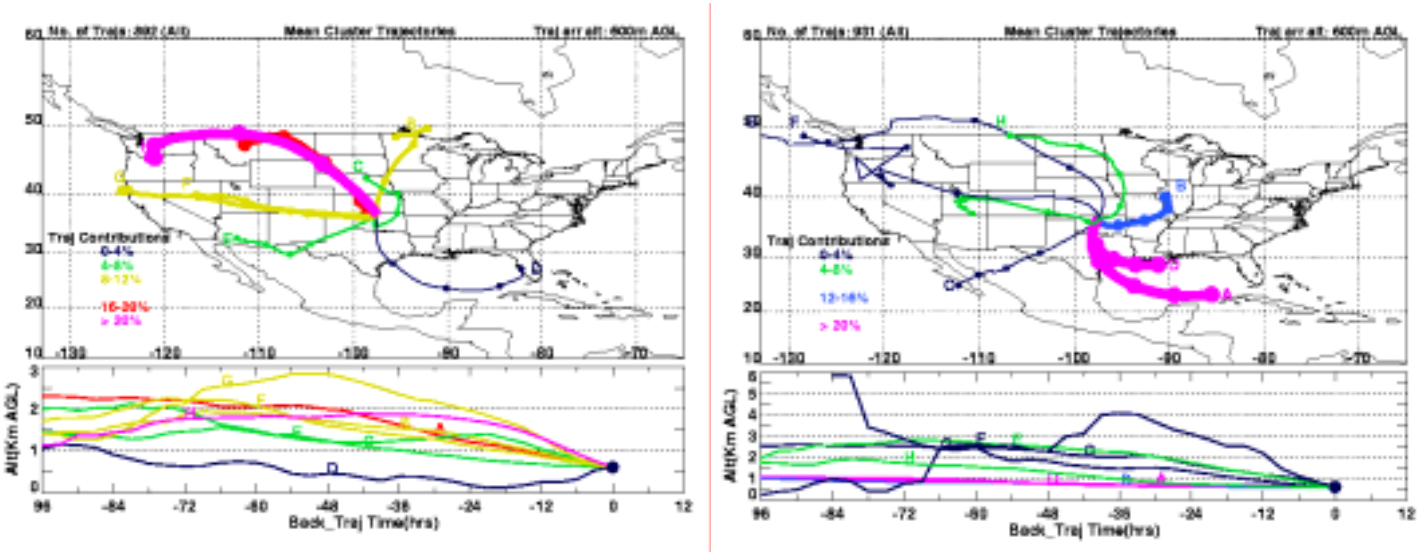

Figure 4. (Left) Mean trajectory clusters for cases when CARL measured PWV <1 cm; (Right) Mean trajectory clusters for cases when CARL measured PWV >3 cm.

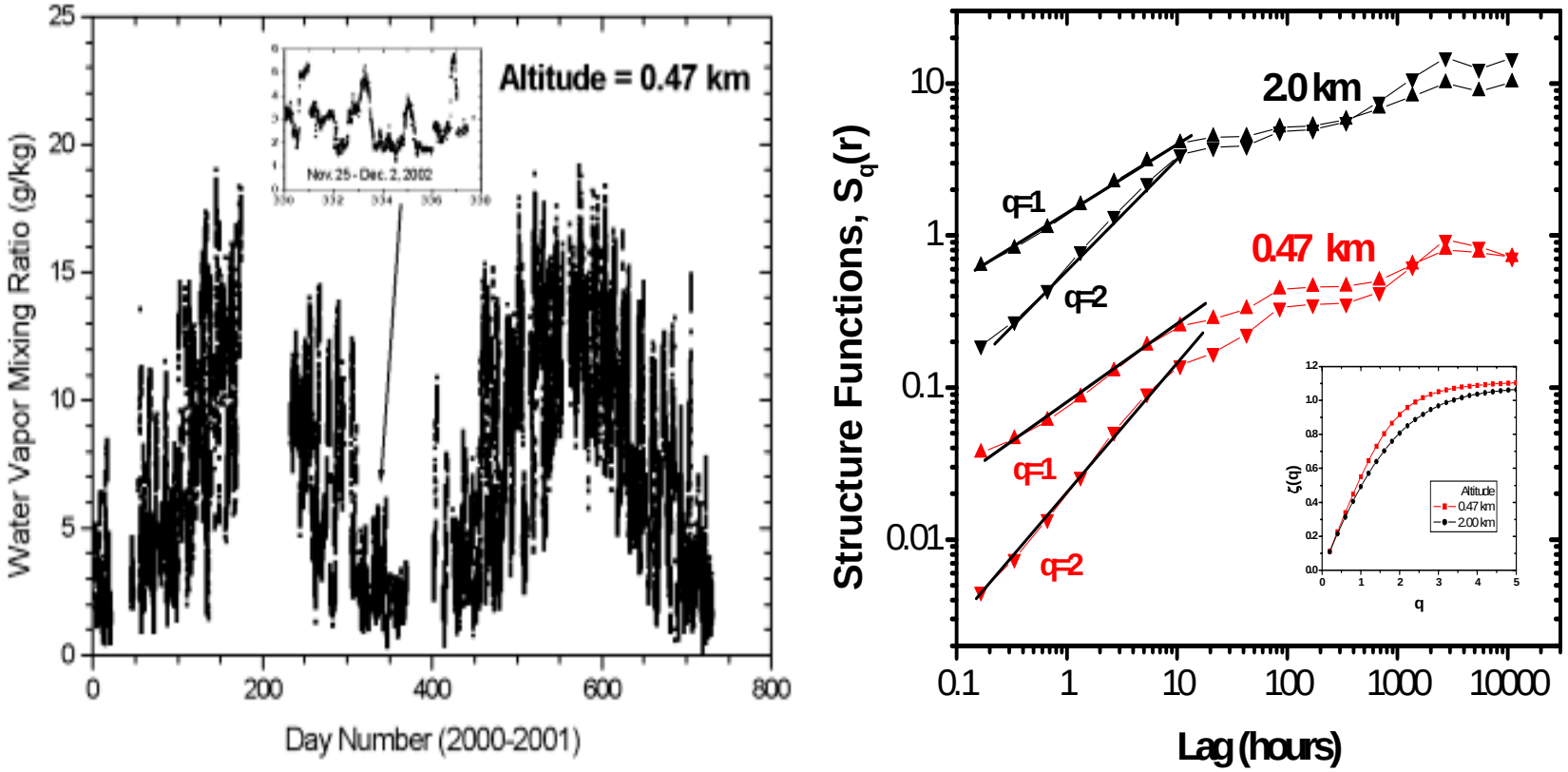

Figure 5. (Left) Times series of water vapor mixing ratio at 0.47 km measured by CARL during 2000-2001. (Right) First and second order structure function and structure function slopes (inset) derived from CARL time series data at 0.47 and 2.0 km.

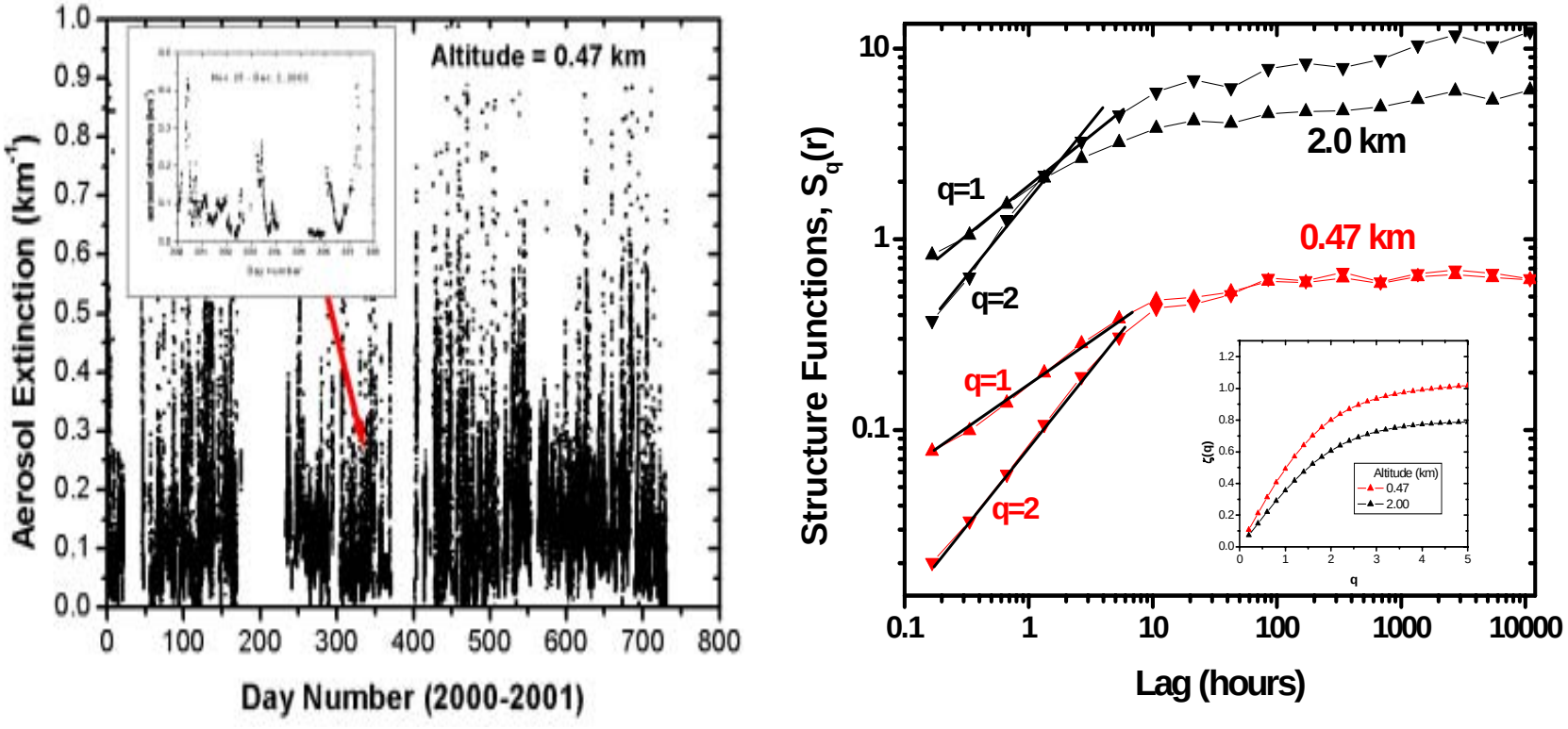

Figure 6. Same as Figure 5 except for aerosol extinction.

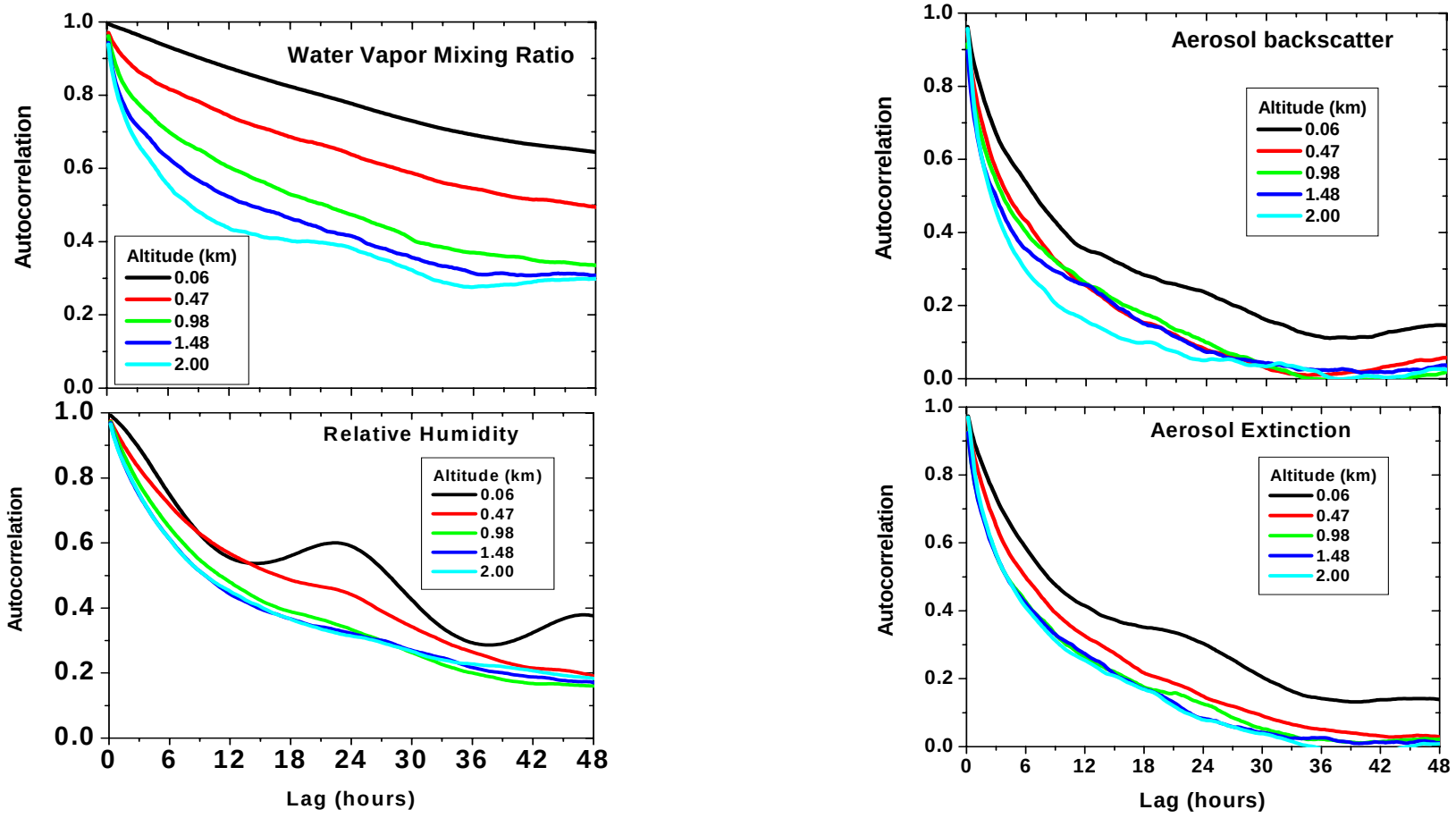

Figure 7. Autocorrelation functions computed using CARL data from 2000-2001.

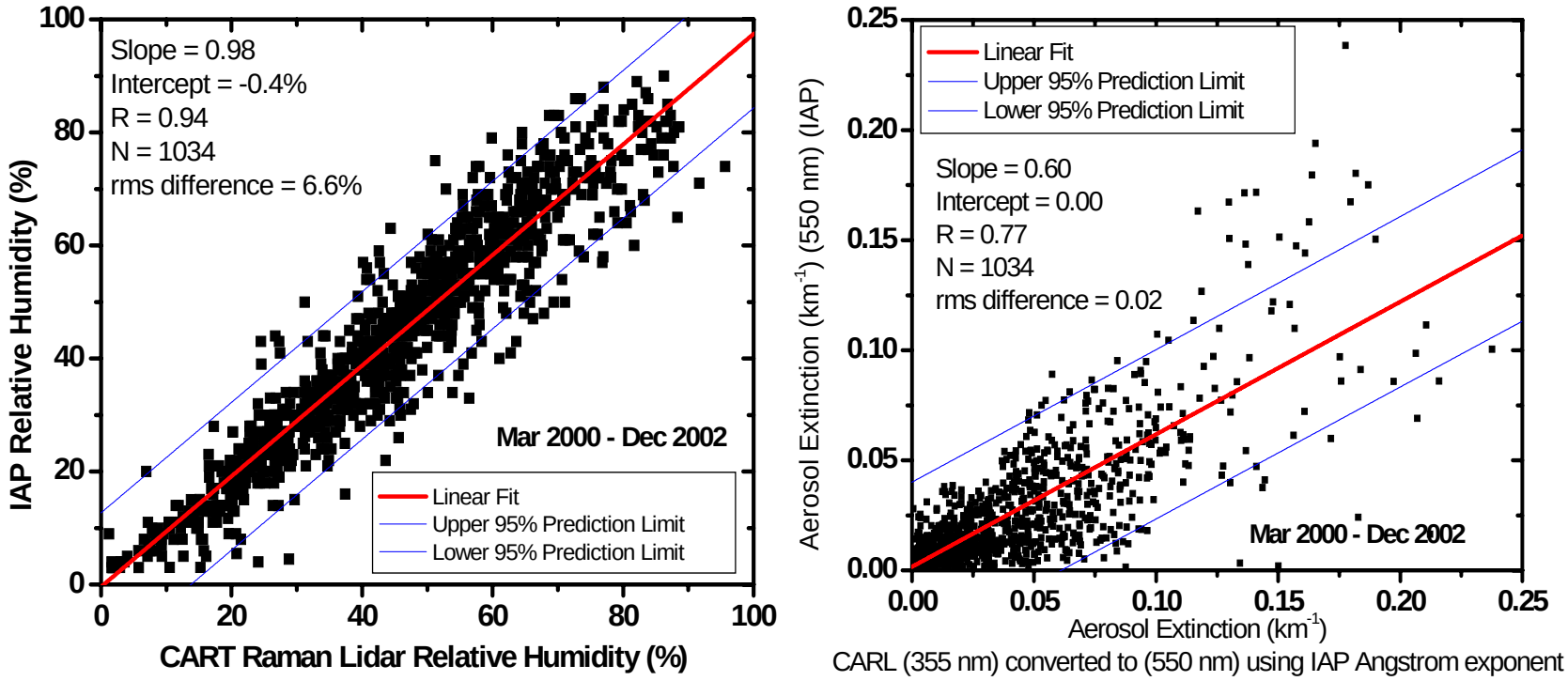

Figure 8. Comparison of relative humidity (left) and aerosol extinction (right) derived from CARL and IAP measurements acquired between 0.15 and 3.7 km.